

3.4 Prediction from Models

Modelling iron limitation in the North Pacific

Kenneth L. Denman^{1,2} and M. Angelica Peña¹

¹ Institute of Ocean Sciences, Fisheries and Oceans Canada, P.O. Box 6000, Sidney, BC, Canada V8L 4B2
E-mail: denmank@pac.dfo-mpo.gc.ca

² Canadian Centre for Climate Modelling and Analysis, University of Victoria, P.O. Box 1700 STN CSC, BC, Canada V8W 2Y2. E-mail: Ken.Denman@ec.gc.ca

Background

The subarctic North Pacific is one of three major high nitrate, low chlorophyll (HNLC) oceanic regions, along with the Southern Ocean and the eastern equatorial Pacific. In these regions, uptake of nitrogen by phytoplankton is widely thought to be regulated by the availability of dissolved iron. The supply of dissolved iron is twofold: via atmospheric deposition of dust and via upward transport of dissolved iron from the ocean interior to the surface euphotic layer. In the subarctic North Pacific, atmospheric deposition has been considered to be the dominant source, despite little compelling evidence.

The subarctic NE Pacific Ocean, in the vicinity of Ocean Station P (OSP), contrasts with the subarctic NW Pacific, because the strong permanent halocline between 100 and 150 m depth in the NE Pacific resists winter mixing deeper than ~120 m and reduces the diffusive upward transport of dissolved nutrients from below the permanent halocline. Long-term observations at OSP, dating back to the 1950s, have given a relatively complete description of the annual cycle in physical properties, nutrients, primary production, phytoplankton chlorophyll, and mesozooplankton. Consequently, a number of modelling studies have used observations from OSP, *e.g.* Evans and Parslow (1985), Frost (1993) and Fasham (1995).

Recent Canadian models with iron limitation

As part of the Canadian JGOFS, GLOBEC and SOLAS studies, we have developed a series of increasingly complex models of the planktonic ecosystem, coupled to a 1-D mixed layer model in the subarctic NE Pacific with simplified regulation of primary production by iron (Denman and Peña, 1999, 2002; Denman, 2003; Peña, 2003; Monahan

and Denman, 2004). In addition, Jeffery (2002) developed an ecosystem model for OSP with a life history representation of copepods. Our models now contain nitrate and ammonium, particulate organic matter (detritus), two size classes of phytoplankton, microzooplankton, and time-dependent grazing by mesozooplankton, specified from 20 years of net tows at OSP. A schematic of the current complexity level of our modelling is shown in Figure 1 (from Peña, 2003), along with the annual cycle for a “standard run” (Fig. 2), with parameter values selected to give results most congruent with long-term observations at OSP. We have used these models to explore ecosystem responses to changes that might accompany climate change: 2° and 5°C warming offsets, and the removal of iron limitation. Generally, these simulations result in large changes in microzooplankton biomass, small changes in phytoplankton biomass, more recycling, and in some cases, changes in export production.

Monahan and Denman (2004) used long-term observations of winds, cloudiness and radiation to develop stochastic forcing functions with statistics (mainly variance and temporal covariability) matching the observations month by month. The model was then run for 1000 years with stochastically varying forcing. With iron limitation characteristic of OSP, the modelled ecosystem annual cycle displayed considerable variability on scales out to decades, but nitrate never became limiting. Simulations of the continental margin (near Line P, Station 04) displayed nitrate limitation most years, and simulations of conditions midway along Line P (~ Station 16) displayed nitrate limitation about 30% of the summers, often for several years at a time. We have added silica into the model and plan to rerun these experiments to see if occasional silica limitation can be simulated at OSP as in observations.

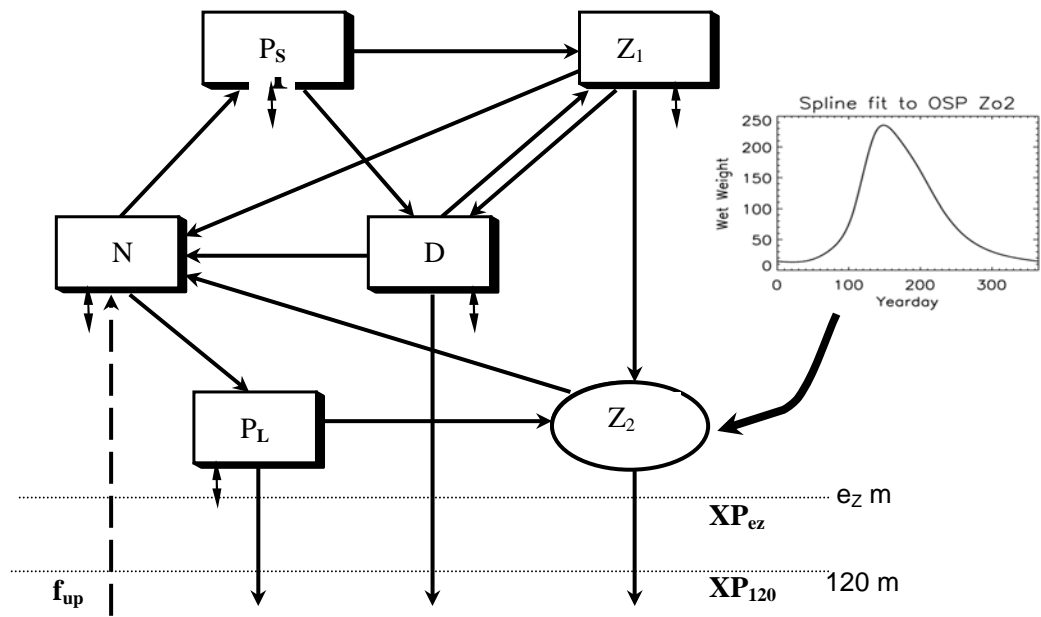


Fig. 1 Schematic diagram of the ecosystem model. Arrows indicate flows of matter through the system, doubled-ended arrows represent mixing fluxes across the base of the euphotic zone and open-ended arrows indicate the input to, and losses from, the system. The export of sinking particles across the base of the euphotic zone and out of the model domain is denoted by XP_{EZ} and XP_{120} . The addition of nitrate in the bottom 5 layers is denoted as f_{up} .

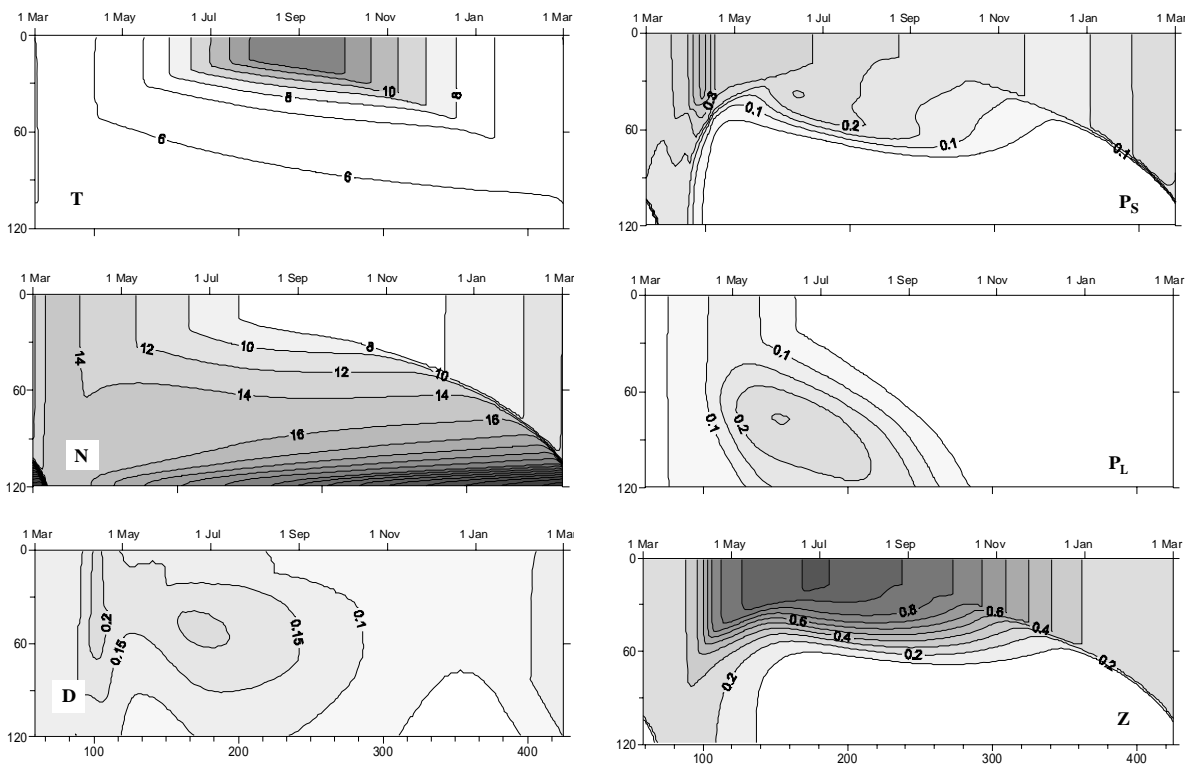


Fig. 2 Time-depth plots for the “standard” run: (left column) temperature ($^{\circ}C$), nitrate and detritus (in $mmol\ N\ m^{-3}$) and (right column) small phytoplankton, large phytoplankton, and microzooplankton (in $mmol\ N\ m^{-3}$).

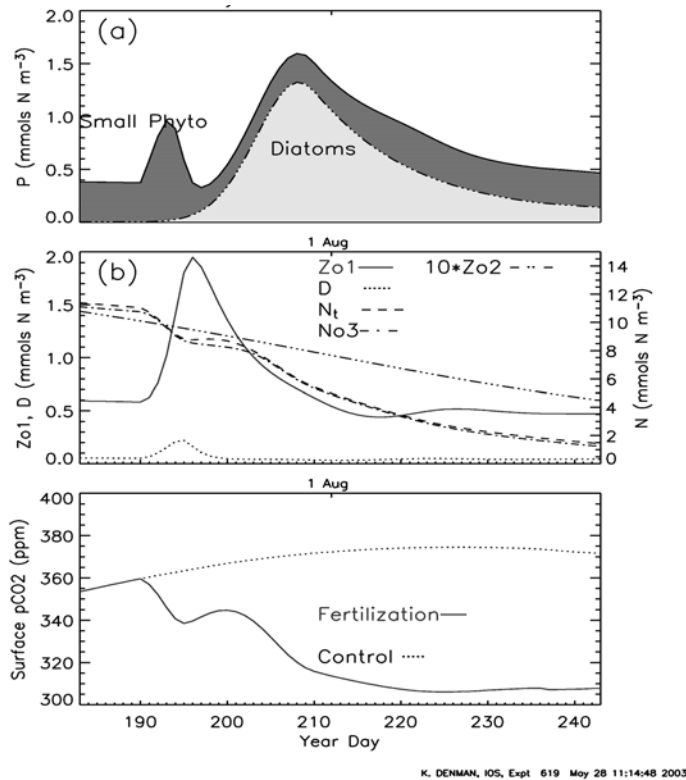


Fig. 3 Preliminary results of Monahan and Denman's ecosystem model for a 20-day fertilization.

Modelling the 2002 SERIES iron fertilization experiment

The ecosystem model described in Monahan and Denman (2004) has been applied to the Subarctic Ecosystem Response to Iron Enrichment Study (SERIES) experiment, with coupling to the inorganic carbon system and just recently to a silica cycle. Preliminary results with the fertilization, lasting 10 or 20 days, capture the main events observed during SERIES: an initial bloom of small phytoplankton followed rapidly by a bloom of microzooplankton, an eventual bloom of large phytoplankton (assumed to be diatoms), the final sinking of diatom aggregates, and the subsurface buildup of ammonium. This sequence of responses of the planktonic ecosystem is shown in Figure 3 for a 20-day fertilization, where the fraction of small phytoplankton assumed to be calcifiers was set to 0.25. The eventual drawdown of CO₂ depends on the length of the bloom and on the fraction of calcifiers. In addition, whether silica becomes limiting towards the end of the bloom depends on the assumed uptake ratio of Si:N.

Future directions

It is clear that for detailed model studies in the subarctic Pacific, a mechanistic model for iron must be developed. For a global model of the ocean carbon cycle to be included in the next generation of the Canadian Global Climate Model, we are trying to balance a detailed representation of processes, such as iron limitation, with the requirement for a model that will represent the "biotic pumps" of carbon over the whole global ocean.

Acknowledgements

We have benefitted from discussions and the work of our coauthors: Jim Christian, Debby Ianson, Nicole Jeffrey, Adam Monahan, and Kos Zahariev.

References

Denman, K.L. 2003. Modelling planktonic ecosystems: parameterizing complexity. *Prog. Oceanogr.* **57**: 429–452.

- Denman, K.L. and Peña, M.A. 1999. A coupled 1-D biological/physical model of the northeast subarctic Pacific Ocean with iron limitation. *Deep-Sea Res. II* **46**: 2877–2908.
- Denman, K.L. and Peña, M.A. 2002. The response of two coupled 1-D mixed layer/planktonic ecosystem models to climate change in the NE subarctic Pacific Ocean. *Deep-Sea Res. II* **49**: 5739–5757.
- Evans, G.T. and Parslow, J.S. 1985. A model of annual plankton cycles. *Biol. Oceanogr.* **3**: 327–347.
- Fasham, M.J.R. 1995. Variations in the seasonal cycle of biological production in subarctic oceans: A model sensitivity analysis. *Deep-Sea Res. I* **42**: 1111–1149.
- Frost, B.W. 1993. A modelling study of processes regulating plankton standing stock and production in the open subarctic Pacific Ocean. *Prog. Oceanogr.* **32**: 17–56.
- Jeffery, N. 2002. Modelling a phytoplankton dichotomy in the eastern subarctic Pacific: Impact of atmospheric variability, iron surface flux, and life cycle dynamics of the Calanoid copepods (*A*) spp., Ph.D. thesis, University of British Columbia, Vancouver, Canada. 154 pp.
- Monahan, A.H. and Denman, K.L. 2004. Impacts of atmospheric variability on a coupled upper-ocean/ecosystem model of the subarctic Northeast Pacific. *Global Biogeochem. Cycles* **18**: GB2010, doi: 10.1029/2003GB002100.
- Peña, M.A. 2003. Modelling the response of the planktonic food web to iron fertilization and warming in the NE subarctic Pacific. *Prog. Oceanogr.* **57**: 453–479.

A proposed model of the SERIES iron fertilization patch

Debby Ianson¹, Christoph Voelker² and Kenneth L. Denman^{1,3}

¹ Institute of Ocean Sciences, Fisheries and Oceans Canada, P.O. Box 6000, Sidney, BC, Canada V8L 4B2
E-mail: ianson@pac.dfo-mpo.gc.ca

² Alfred Wegener Institute for Polar Marine Research, Am Handelshafen 12, 27570 Bremerhaven, Germany

³ Canadian Centre for Climate and Modelling Analysis, University of Victoria, P.O. Box 1700 STN CSC, BC, Canada V8W 2Y2

Introduction

Artificial iron fertilization experiments have shown that the micronutrient, iron, limits phytoplankton growth in high nutrient, low chlorophyll (HNLC) regions of the ocean (Martin and Fitzwater, 1988). It is assumed that episodic aeolian iron input to HNLC regions causes phytoplankton blooms that afterwards decline quickly. It is difficult to predict when such events will occur, so they have rarely been observed (mainly in sediment trap data).

Iron fertilization experiments allow the response of the natural system to iron addition to be studied. Besides confirming the hypothesis of iron limitation in HNLC regions, they have shown that iron often has a short residence time in the surface layer due to particle scavenging and biological uptake. In recent years the complex chemical cycling of iron in the ocean has been recognized as an additional controlling factor (Wells, 2003). However, this cycling remains poorly understood.

The species composition of phytoplankton in nutrient (including iron) replete conditions shifts to a diatom-based population. Diatoms require silicic acid, so their dominance will alter the macronutrient balance. Remineralization (dissolution) length scales of silicic acid are thought to be longer than those of nitrogen and phosphorus. Thus iron fertilization causes changes in biological community structure and the chemistry of the water column. Here, we propose a model, constrained by the subarctic ecosystem response to iron enrichment (Subarctic Ecosystem Response to Iron Enrichment Study – SERIES) data, to investigate the biogeochemical pathways of iron, nitrogen, silicic acid and carbon in the euphotic zone after a large and sudden introduction of dissolved iron.

Experiment

The SERIES experiment and results are described in detail in other papers in this report. Briefly, three ships occupied the fertilized patch over a 25-day period. The patch was tracked using the tracer, sulphur hexafluoride (SF₆). Diatom growth was exponential until iron became limiting. However, the diatom seed population was small so that initially the non-diatom species present prior to iron addition showed the largest response. The latter phase of the bloom was dominated by oceanic diatoms. Silicic acid became limiting to diatom growth before nitrogen and observations suggest that silica dissolution may be occurring at shallower depths relative to nitrogen than previously thought.

Station P (50°N, 145°W) is argued to be an excellent site for such experiments, having relatively homogeneous water properties in the horizontal. During the experiment, however, the patch sat on a strong east–west frontal gradient so that outer waters were not uniform in nutrient or salinity concentrations. In addition, the patch appears to have slipped over a distinctly different water mass in the later course of the experiment. These physical changes make it more difficult to estimate dilution or entrainment fluxes from the patch in both the vertical and the horizontal. We have designed our model to address this difficulty.

Model

The model consists of three components: physical, ecological and the iron component. Below, we discuss the physical and iron aspects of the model. We will use the ecological model of Denman (2003; also Denman and Peña, this report). Iron, carbon, nitrogen and silicic acid will be tracked as model currencies. In addition, salinity and SF₆ will be tracked to constrain the physical parameters.

Physical

We model three physical regions separated by transition zones having linear gradients in model properties. Each region is assumed to be homogeneous in properties. The main region, the inside of the patch (region 1), is described by its area, perimeter and depth, all of which are prescribed to vary in time according to the observations (Fig. 1). The depth is the mixed layer depth (MLD) (Steiner *et al.*, in press). The horizontal parameters are based on the SF₆ data (Law *et al.*, in press). The area and movement of the MLD determine vertical entrainment and mixing. The MLD and the change in the perimeter determine the horizontal exchange. The remaining regions are the surrounding surface waters (region 2) and the lower layer (region 3) (Fig. 1b). Concentrations of model quantities in regions 2 and 3 will be prescribed, varying in time, based on observations.

Iron

Iron in seawater exists in a variety of chemical and physical forms, including dissolved organic complexes, colloidal and particle-bound forms. This speciation influences the residence time of iron within the mixed layer, as some forms are more readily lost from the euphotic zone by adsorbing onto sinking particles than others (Bowie *et al.*, 2001; Wu and Boyle, 2002). Because some iron species are more easily taken up by phytoplankton than others (*e.g.*, Hutchins *et al.*, 1999), speciation might also influence the bioavailability of iron.

Iron speciation for SERIES is reported in terms of operationally defined categories by filtration procedures. To make the model as consistent as possible with the observations, the model differentiates between truly dissolved, colloidal and particulate iron. The dissolved pool is further split into inorganic ferric iron Fe(III)', which includes all hydrolyzed species of Fe(OH)_n³⁻ⁿ, dissolved inorganic ferrous iron Fe(II)', and organically complexed iron FeL.

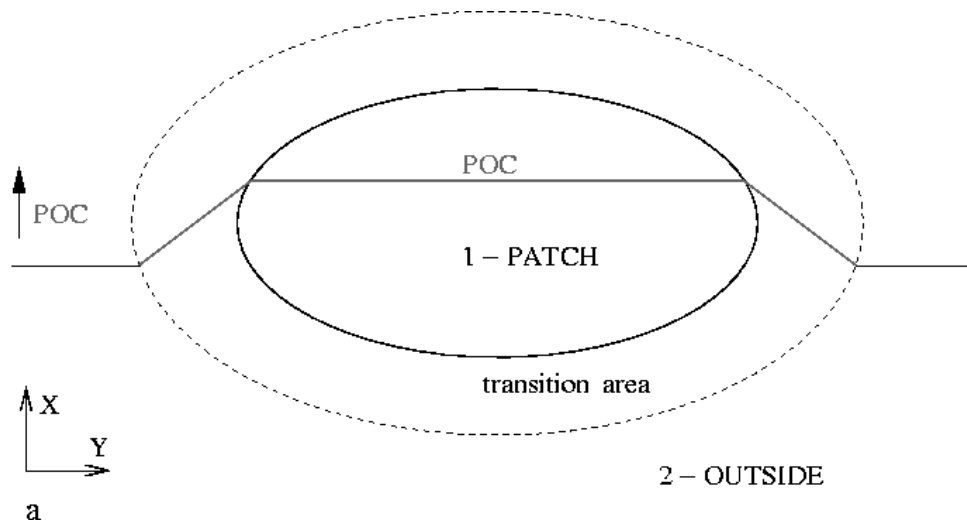


Fig. 1 The physical model structure in the horizontal showing the state variable particulate organic carbon (POC) in region 1 (the patch), region 2 (the outside) and the transition area between (a) and the vertical showing salinity (S) in the upper (region 1, the patch) and lower (region 3) layer with the transition between (b).

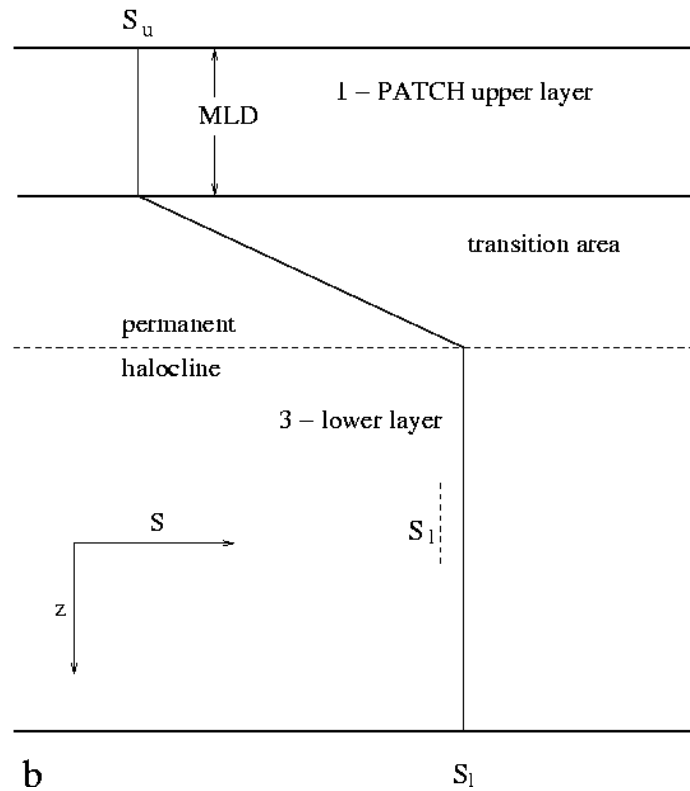


Fig. 1 Continued.

A number of processes are known to convert iron in seawater from one of these forms into another. The model includes the processes of:

- complex formation and dissociation involving organic ligands (*e.g.*, Witter *et al.*, 2000);
- photoreduction of the different iron forms, both directly (*e.g.*, Barbeau *et al.*, 2003) and indirectly by photoproduced superoxide (Voelker and Sedlak, 1995);
- oxidation of Fe(II)' by oxygen, superoxide and hydrogen peroxide (*e.g.*, Millero and Sotolongo, 1989);

- scavenging onto particles (Nyffeler *et al.*, 1984);
- colloid formation (Johnson *et al.*, 1994);
- colloid aggregation (Wen *et al.*, 1997).

We assume that the fast reactions transforming iron between the three dissolved forms are in instantaneous equilibrium, such that the speciation of dissolved iron can be calculated diagnostically (Fig. 2).

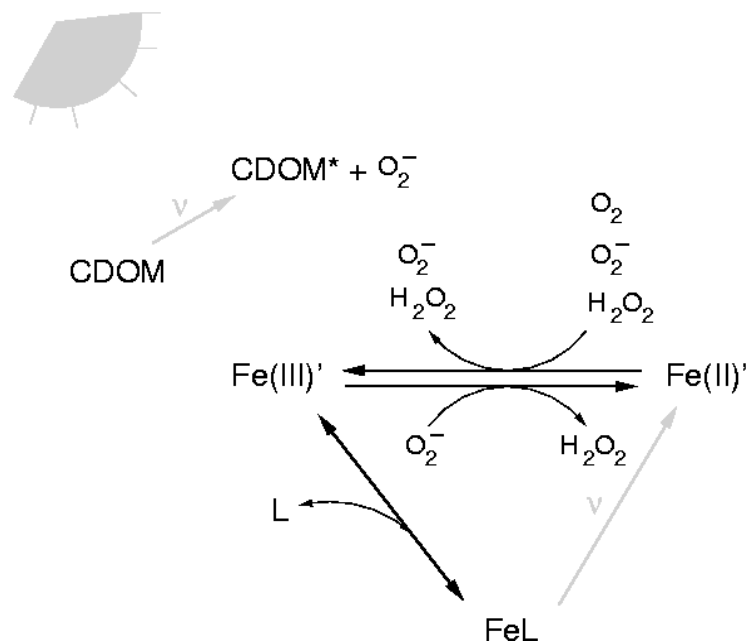


Fig. 2 The diagnostic portion of the iron model showing the species of dissolved iron and their transformations. Photoproduction of O₂⁻ from coloured dissolved organic matter (CDOM) causes reduction of Fe(III)'.

References

- Barbeau, K., Rue, E., Trick, C., Bruland, K. and Butler, A. 2003. Photochemical reactivity of siderophores produced by marine heterotrophic bacteria and cyanobacteria based on characteristic Fe(III) binding groups. *Limnol. Oceanogr.* **48**: 1069–1078.
- Bowie, A., Maldonado, M., Frew, R., Croot, P., Achterberg, E., Mantoura, R., Worsfold, P., Law, C. and Boyd, P. 2001. The fate of added iron during a mesoscale fertilization experiment in the Southern Ocean. *Deep-Sea Res. II* **48**: 2703–2743.
- Denman, K.L. 2003. Modelling planktonic ecosystems: parameterizing complexity. *Prog. Oceanogr.* **57**: 429–452.
- Hutchins, D., Witter, A., Butler, A. and Luther III, G. 1999. Competition among marine phytoplankton for different chelated iron species. *Nature* **400**: 858–861.
- Johnson, K., Coale, K., Elrod, V. and Tindale, N. 1994. Iron photochemistry in seawater from the equatorial Pacific. *Mar. Chem.* **46**: 319–334.
- Law, C.S., Crawford, W., Smith, M., Boyd, P.W., Wong, C.S., Nojiri, Y., Robert, M., Abraham, E.R., Johnson, W.K. and Arychuk, M. 2006. Patch evolution and the biogeochemical impact of entrainment during an iron fertilisation experiment in the sub-Arctic Pacific. *Deep-Sea Res. II*, in press.
- Martin, J. and Fitzwater, S. 1988. Iron deficiency limits phytoplankton growth in the northeast Pacific subarctic. *Nature* **331**: 341–343.
- Millero, F. and Sotolongo, S. 1989. The oxidation of Fe(II) with H₂O₂ in seawater. *Geochim. Cosmochim. Acta* **53**: 1867–1873.
- Nyffeler, U., Li, Y.-H. and Santschi, P. 1984. A kinetic approach to describe trace-element distribution between particles and solution in natural aquatic systems. *Geochim. Cosmochim. Acta* **48**: 1513–1522.
- Steiner, N., Denman, K., McFarlane, N. and Solheim, L. 2006. Simulating the coupling between atmosphere–ocean processes and the planktonic ecosystem during SERIES. *Deep-Sea Res. II*, in press.
- Voelker, B. and Sedlak, D. 1995. Iron reduction by photoproduced superoxide in seawater. *Mar. Chem.* **50**: 93–102.
- Wells, M. 2003. The level of iron enrichment required to initiate diatom blooms in HNLC waters. *Mar. Chem.* **82**: 101–114.
- Wen, L.-S., Santschi, P. and Tang, D. 1997. Interactions between radioactively labeled colloids and natural particles: Evidence for colloidal pumping. *Geochim. Cosmochim. Acta* **61**: 2867–2878.
- Witter, A., Hutchins, D., Butler, A. and Luther III, G. 2000. Determination of conditional stability constants and kinetic constants for strong model Fe-binding ligands in seawater. *Mar. Chem.* **69**: 1–17.
- Wu, J. and Boyle, E. 2002. Iron in the Sargasso Sea: Implications for the processes controlling dissolved Fe distribution in the ocean. *Global Biogeochem. Cycles* **16**: DOI 10.1029/2001GB001453.